

# Detection of rubber particle cavitation in toughened plastics using thermal contraction tests

C.B. Bucknall<sup>a,\*</sup>, D.S. Ayre<sup>a</sup>, D.J. Dijkstra<sup>b</sup>

<sup>a</sup>*Advanced Materials Department, Cranfield University, Bedford MK43 0AL, UK*

<sup>b</sup>*Bayer AG, Central Research, Physics Department, D-51368 Leverkusen, Germany*

Received 2 June 1998; received in revised form 25 August 1999; accepted 2 November 1999

---

## Abstract

Uniaxial thermal contraction/expansion tests were carried out below 40°C on poly(styrene-*co*-acrylonitrile) (PSAN) and acrylonitrile–butadiene–styrene (ABS) specimens. In PSAN, contraction and expansion were reversible and linear with temperature. By contrast, some ABS materials underwent an irreversible volumetric expansion over a temperature interval of ~30 K, which was superimposed on the ordinary thermal contraction. On subsequent reheating and cooling in the temperature range –80 to +40°C, expansion and contraction in these ABS polymers followed an approximately linear path, but after annealing at 105°C the specimen again exhibited an S-shaped thermal contraction curve. It is concluded that the anomalous contraction behaviour observed during initial cooling is due to cavitation of the rubber particles, which results in a relaxation of thermally induced tensile stresses within the rubber phase, and a corresponding fall in the coefficient of expansion of ABS. Analysis of thermal expansion data provides a method for estimating the volume fraction of rubber particles that have cavitated, and shows that void formation is controlled by an energy barrier. The data suggest that the void formation energies required to surmount this barrier are comparable with those of the naturally occurring voids that constitute the free volume. The effects of rubber particle cavitation on yielding were studied by cooling ABS specimens to sub-zero temperatures, and then subjecting them to creep tests at 23°C. It was found that cooling caused a progressive increase in the creep rate, which was ten times faster in ABS cooled to –60°C than in uncooled ABS. © 2000 Elsevier Science Ltd. All rights reserved.

*Keywords:* Cavitation; Rubber toughening; Thermal contraction

---

## 1. Introduction

Cavitation of rubber particles was first observed in toughened plastics over 20 years ago [1], and the phenomenon has since been observed in a wide range of rubber-toughened polymers. Two recent publications provide reviews of the relevant literature [2,3]. Most of the published evidence comes from optical or electron microscope studies of cavities that formed within the rubber phase when the polymer was subjected to large tensile stresses. These conditions almost invariably produce a substantial amount of shear yielding and/or crazing in the surrounding rigid matrix, which limits the effectiveness of microscopy as an observational technique in two important ways: (a) by the time they are examined in the microscope, the cavities have already undergone large expansions from their original equilibrium dimensions, in response to the increasing local strains in the matrix; and (b) it is difficult to determine whether yielding takes place in the matrix before or after cavitation in the

rubber particles. Thus, while microscopy has obvious advantages in that it allows direct observation and characterisation of morphology of the cavities formed within rubber particles, there is a clear need for alternative experimental techniques that can detect and monitor the cavitation process itself during its early stages.

The present paper addresses this problem. Its aim is to demonstrate four important principles: (a) that cooling of unstressed specimens provides a method for initiating rubber particle cavitation under conditions that do not simultaneously produce yielding in the matrix phase; (b) that simple thermal contraction–expansion measurements are capable of detecting and quantifying the extent of rubber particle cavitation while it is taking place; (c) that the technique offers considerable insight into the mechanism of void initiation; and (d) that the enhanced levels of rubber particle cavitation that are induced by prior cooling cause a significant increase in deformation rates when the specimen is subjected to tensile stress. The materials chosen for this study are various grades of acrylonitrile–butadiene–styrene (ABS) polymers.

---

\* Corresponding author.

Between  $T_{gm}$ , the glass transition temperature of the poly(styrene-*co*-acrylonitrile) (PSAN) matrix (subscript m), and  $T_{gr}$ , the glass transition temperature of the diene rubber (subscript r), the two phases of ABS have very different coefficients of thermal expansion. Typical values for the volumetric expansion coefficient are  $\beta_m = 1.8 \times 10^{-4} K^{-1}$  for both polystyrene (PS) and PSAN, and  $\beta_r = 7.6 \times 10^{-4} K^{-1}$  for polybutadiene [4]. Consequently, addition of quite small amounts of rubber to PSAN can raise its coefficient of expansion appreciably; a typical ABS polymer containing 15 wt% rubber has  $\beta_{ABS} = 2.7 \times 10^{-4} K^{-1}$ , about 50% higher than that of PSAN [5]. In order to produce changes of this magnitude in the thermal contraction behaviour of ABS, the rubber must develop substantial internal tensile stresses, which increase as the ABS is cooled from  $T_{gm}$  ( $\sim 100^\circ C$ ). Within homogeneous spherical rubber particles, these stresses take the form of pure hydrostatic tension, which produces radial stresses acting inwards on the surrounding shell of matrix. These are balanced by compressive hoop stresses in the shell, which act tangentially to the particle-matrix boundary. This combination of stresses causes the shell of matrix surrounding the particle to contract to a smaller volume than it would occupy in the unstressed state.

It is obvious that polybutadiene can affect the thermal contraction of ABS in this way only if the rubber particles remain intact. Subject to this condition, the effects of rubber particles on the expansion behaviour of ABS, and the changes resulting from cavitation, can be quantified using the following equation for  $\beta_{ABS}$ , which is given in a slightly different form by Boyce et al. [6]:

$$\beta_{ABS} = \beta_m + (\beta_r - \beta_m)\phi \left[ \frac{4G_m K_p + 3K_m K_p}{4G_m K_m (1 - \phi) + K_p (4G_m \phi + 3K_m)} \right] \quad (1)$$

where  $G_m$  and  $K_m$  are, respectively, the shear and bulk moduli of the matrix,  $K_p$  is the bulk modulus of the particle, and  $\phi$  is the volume fraction of intact, well-bonded rubber particles. The term in square brackets is relatively insensitive to  $\phi$ . For example, if  $G_m$ ,  $K_m$  and  $K_p$  are assigned typical values of 1.2, 4.0 and 2.0 GPa, respectively, this term varies from 0.80 at  $\phi = 0.10$  to 0.82 at  $\phi = 0.25$ . Consequently, Eq. (1) can be written, to a good approximation:

$$\beta_{ABS} = \beta_m + 0.81\phi(\beta_r - \beta_m). \quad (2)$$

As the toughened polymer is cooled, the triaxial tensile stresses in the rubber phase, which are responsible for this increase in  $\beta_{ABS}$ , can eventually become large enough to cause either cavitation or debonding [7]. In the limit, cohesive or adhesive failures of this type might reduce  $K_p$  to zero, so that  $\beta_{ABS}$  becomes equal to  $\beta_m$ , the expansion coefficient of PSAN.

Work by Lazzeri, Bucknall and co-workers has shown

that the limiting factor in rubber particle cavitation is not the absolute level of triaxial tension acting on the rubber, but the amount of energy available for the formation of the incipient void. This in turn is dependent on the volume strain energy density in the rubber phase, the size of the particle, the shear modulus and surface energy of the rubber phase, and the potential energy stored in the surrounding shell of rigid matrix phase [8,9]. Calculations based on this model show that, for many toughened plastics, simply cooling the material from  $T_{gm}$  to  $T_{gr}$  should provide more than enough energy to cause cavitation in some or all of the rubber particles.

This conclusion is supported by earlier evidence from dynamic mechanical tests on ABS polymers, which in some cases show splitting of the low temperature  $\tan \delta$  peak associated with the glass transition in the rubber phase [10–12]. On the basis of this evidence, it is clear that cavitated particles produce a loss peak close to the glass transition  $T_{gr}$  of the fully-relaxed rubber, whereas intact particles produce a loss peak approximately 10 K lower in temperature. The downward shift in peak temperature observed in intact particles is due to an increase in the free volume of the rubber phase as the ABS is cooled and a state of pure triaxial tension develops inside the particles. Cavitation relaxes these internal stresses, allowing the rubber to contract towards its equilibrium, unstressed density. When the populations of intact and cavitated particles are roughly equal, a split peak can be observed quite clearly.

## 2. Experimental

The materials used for this study were a PSAN consisting of 65 wt% styrene and 35 wt% acrylonitrile, and two ABS polymers: ABS 16, which contains 16 vol% polybutadiene (with  $T_{gr} \sim -90^\circ C$ ) and a trace of silicone oil, and ABS 27, which contains 27 vol% of a different polybutadiene ( $T_{gr} \sim -75^\circ C$ ), but no silicone oil. The locations of the two glass transition temperatures are important, because cavitation of the particles requires a low value for  $G_r$ , the shear modulus of the rubber phase [2,3,8,9], and  $G_r$  rises steeply as the rubber is cooled into the region of its  $T_{gr}$ . Thus, the ultimate limits on thermally induced cavitation in ABS are  $T_{gm}$ , above which there are no thermal contraction stresses at the particle-matrix boundary, and  $T_{gr}$ , below which the rubber is too rigid to cavitate.

A further material, ABS 13, was prepared for this study by melt compounding ABS 27 with PSAN and 0.1% silicone oil in a twin-screw extruder, to give an ABS with a final rubber content of 13 vol%, which in its composition resembled ABS 16. The reason for choosing three ABS polymers, containing different concentrations of rubber and additives, was to demonstrate that anomalous thermal contraction behaviour is not specific to one grade of ABS, and that it is affected by the various factors that are known to

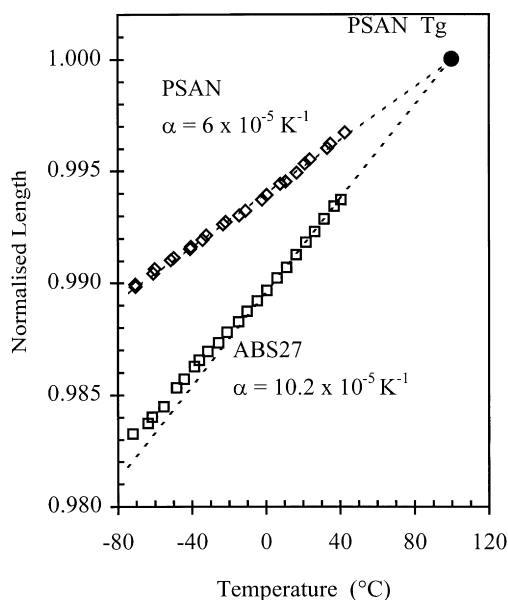


Fig. 1. Thermal contraction data for compression moulded PSAN and ABS 27. The reference length  $L_0$  for both specimens is defined at  $100^\circ\text{C}$  (taken as the  $T_g$  of PSAN). Lower construction line calculated using Eq. (1), with  $\phi = 0.27$ .

influence rubber particle cavitation. Decreasing the rubber content increases the mechanical constraints that are imposed by the matrix on thermal contraction in the rubber particles, but makes observations more difficult by reducing the size of the corresponding loss peak [10,11]; ABS polymers containing 10–15% rubber represent a compromise between these tendencies. Silicone oil was added to ABS 13 because of previous evidence that certain liquid additives promote rubber particle cavitation in ABS [11].

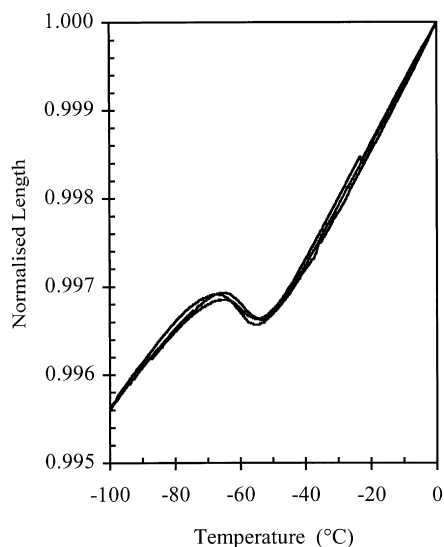


Fig. 2. Thermal contraction behaviour of three fresh specimens of ABS 16 cut from an 8 mm injection moulded plaque, and tested in the  $x$  (flow),  $y$  and  $z$  directions. Data for each specimen normalised to its reference length  $L_0$  at  $0^\circ\text{C}$ .

Both laboratories involved in this project contributed to the experimental programme. In the first series of measurements, specimens measuring  $4 \times 4 \times 8$  mm were machined from 8 mm thick injection-moulded plaques of ABS 16. Thermal contraction and expansion experiments were carried out on these samples under a nitrogen purge at a cooling rate of  $1 \text{ K min}^{-1}$ , using a Perkin–Elmer DMA7 machine with liquid nitrogen coolant. During each test, a 20 mN compressive load was applied to the specimens by means of a 3 mm diameter brass rod. In the second series of tests, rectangular bars measuring  $120 \times 5 \times 3$  mm were machined from compression moulded ( $200^\circ\text{C}$ ) plaques of ABS 13 and injection moulded plaques of ABS 16, both of 3 mm thickness. The ABS 16 specimens were first annealed at  $105^\circ\text{C}$  to relieve internal stresses generated during injection moulding. Thermal contraction measurements were then made by cooling the bars at a moderate rate (also  $\sim 1 \text{ K min}^{-1}$ ), under an axial compressive load of 5 N, in the specimen chamber of a Gabo Eplexor dynamic mechanical thermal spectrometer (DMTS) fitted with a displacement transducer.

Transmission electron microscopy was used to confirm the presence of voids in thermally conditioned ABS specimens. After being cooled to the chosen temperature and returned to room temperature, specimens were faced, stained with osmium tetroxide, and sectioned using a Reichert–Jung ultramicrotome fitted with a diamond knife.

The effects of particle cavitation on deformation behaviour were studied by cooling tensile specimens of ABS 13 to  $-20$ ,  $-40$  and  $-60^\circ\text{C}$ , warming them back to room temperature, and subjecting each specimen to a tensile creep test at  $23^\circ\text{C}$  under an applied stress of 34.5 MPa.

### 3. Results

Fig. 1 compares the thermal contraction behaviour of PSAN and ABS 27 between  $40$  and  $-80^\circ\text{C}$ . In this diagram, the data are normalised with respect to the (extrapolated) reference length of the sample at  $100^\circ\text{C}$ , which is the  $T_g$  of PSAN; i.e.  $L_{\text{rel}} = L/L_0 = L(T)/L(T_{\text{gm}})$ . It is assumed that the PSAN matrix of ABS is soft and fully relaxed at this temperature, so that the stresses acting at the particle–matrix interface are zero. Cooling below this temperature then sets up tensile stresses normal to the interface in both phases. The dotted line through the ABS data follows Eq. (1), with the modulus values given in Section 1, and  $\phi = 0.27$ . This fit indicates that the rubber particles in ABS 27 remain effectively intact between  $40$  and  $0^\circ\text{C}$ . If any significant amount of cavitation had taken place in the ABS, the slope of the line would be lower in this temperature range. Below  $0^\circ\text{C}$ , there is a small deviation from the dotted line. The significance of this observation will be reviewed later, in the light of measurements on other ABS polymers.

Results from three separate cooling experiments on samples cut from an 8 mm thick injection-moulded plaque

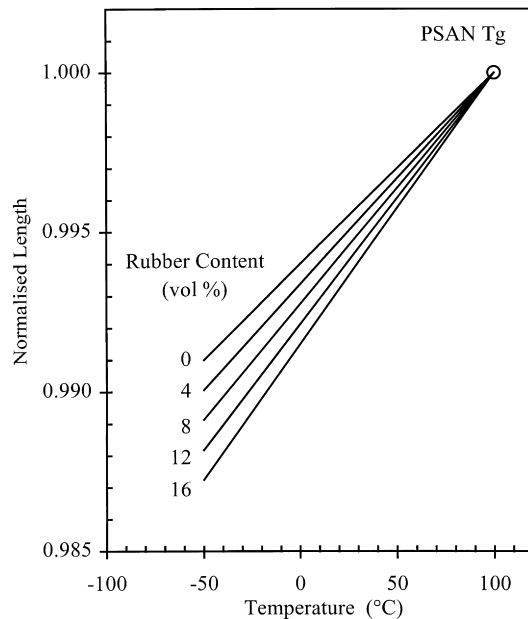


Fig. 3. Experimental expansion-contraction curve for PSAN (0% rubber) compared with calculated curves for ABS containing 4, 8, 12 and 16 vol% of intact rubber particles, obtained using Eq. (1). Cavitation reduces the concentration of intact rubber particles, and shifts the expansion curve upwards.

of ABS 16 are presented in Fig. 2. Each test was performed on a fresh specimen, and strains were measured along axes lying parallel ( $x$ ) or normal ( $y, z$ ) to the flow direction. There is good agreement between measurements made in the three directions, indicating that the results are reproducible, and that the thermal contraction behaviour of the mouldings is essentially isotropic, although there is inevitably a certain amount of orientation in injection moulded bars. In each cooling experiment, the thermal contraction curve is linear between 0 and  $-45^{\circ}\text{C}$ , passes through a distinctly non-linear S-shaped section between  $-45$  and  $-75^{\circ}\text{C}$ , then resumes a

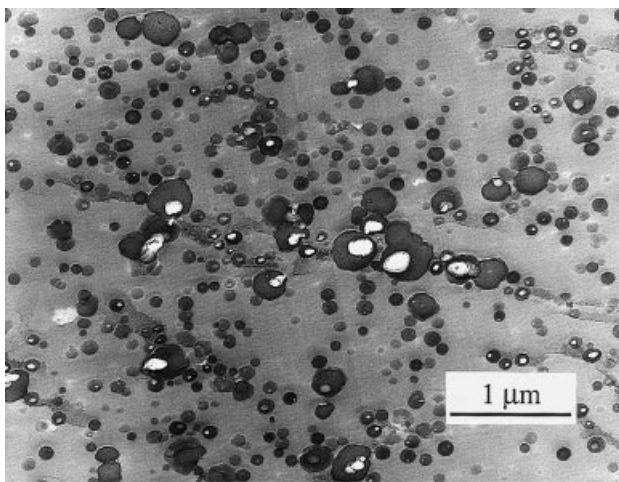


Fig. 4. Thin section of osmium-stained ABS 13, showing cavitation in rubber particles.

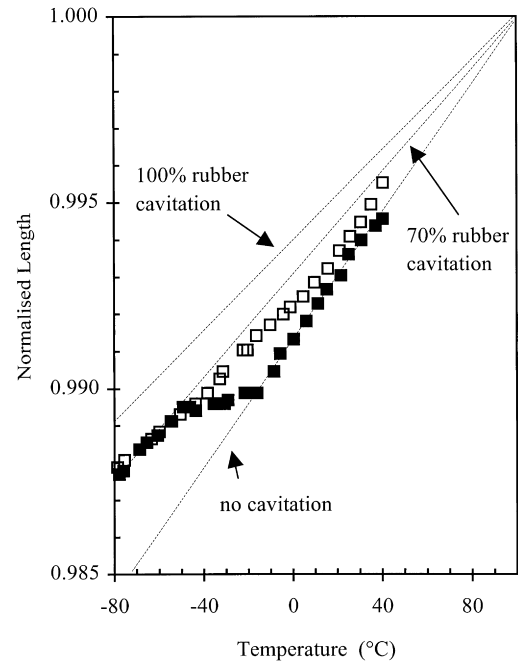


Fig. 5. Thermal contraction and expansion behaviour of an annealed specimen of ABS 16, showing anomalous behaviour during cooling (■), and approximately linear thermal expansion during subsequent heating (□). Reference length  $L_0$  defined as the length at  $100^{\circ}\text{C}$  during initial cooling. Construction lines calculated as in Fig. 3.

linear course, with reduced slope, below  $-75^{\circ}\text{C}$ . Extrapolation of the initial, linear, part of the contraction curve provides a baseline for comparison of the low-temperature data. The observed deviation from a straight line represents an expansion of the ABS, relative to the baseline, throughout the temperature interval from  $-45$  to  $-75^{\circ}\text{C}$ . This expansion can occur only as a result of cavitation in the rubber particles or debonding at the particle-matrix boundary.

The reduced slope between  $-75$  and  $-100^{\circ}\text{C}$ , corresponding to a reduction in the thermal expansion coefficient, is another indication of rubber particle cavitation. This point is illustrated schematically in Fig. 3, which compares the observed contraction behaviour of PSAN (0% rubber) with that of ABS materials containing 4, 8, 12 and 16 vol% of polybutadiene. The lines representing ABS polymers were calculated using Eq. (1), with the values for moduli quoted Section 1. It is important to note that the line labelled '8% rubber' applies not only to an ABS containing 8% rubber particles, all of which are intact, but also to an ABS containing 16 vol% rubber particles, half of which have cavitated.

In order to confirm that anomalous contraction behaviour is not specific to ABS 16, cooling experiments were also carried out on the other ABS polymers listed Section 2. Similar marked deviations from linearity were observed in ABS 13, whereas ABS 27, the source of the rubber particles in ABS 13, showed only a minor deviation from linearity, as shown in Fig. 1. It was concluded that reducing the rubber content by blending with PSAN, and (more importantly)

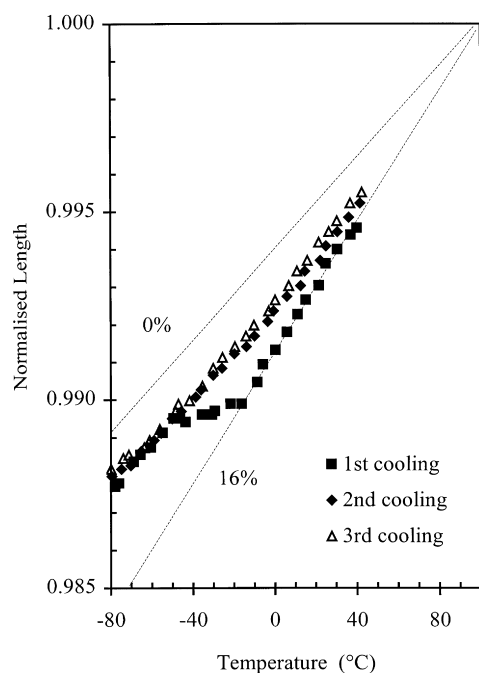


Fig. 6. Contraction behaviour of ABS 16 during first, second and third cooling cycles between +40 and  $-80^{\circ}\text{C}$ . Construction lines are for PSAN and ABS containing 16 vol% intact particles, from Fig. 3.

adding a trace of silicone oil, facilitated rubber particle cavitation on cooling. Methods for assessing the relative importance of the two factors are discussed later in this paper.

The presence of cavitated particles in thermally conditioned ABS was confirmed using TEM, as illustrated in Fig. 4. This micrograph shows a relatively thick section cut from a specimen of ABS 13, which was pre-cooled to  $-60^{\circ}\text{C}$ , held at that temperature for 30 min, returned to room temperature, and stained with osmium tetroxide. Image analysis gives a value of about 60 vol% as the fraction of rubber particles containing single voids. Only a few

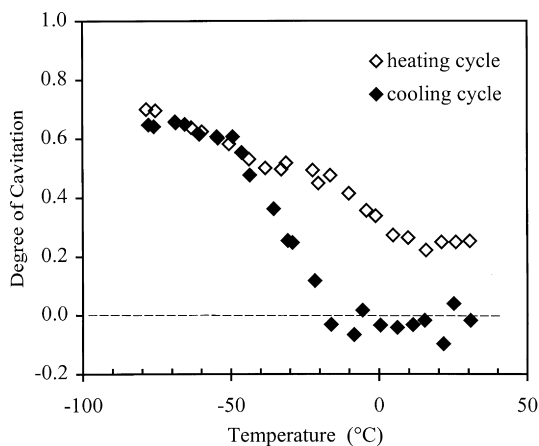


Fig. 7. Effective degree of cavitation in ABS 16 during first cooling and reheating cycle, calculated using method illustrated in Fig. 3.

voids were observed in samples of ABS 13 that had not been cooled below  $-20^{\circ}\text{C}$ .

When ABS 16 was reheated to  $23^{\circ}\text{C}$ , the expansion curve was approximately linear rather than S-shaped, as shown in Fig. 5, indicating that cavitation below  $T_{\text{gm}}$  is irreversible and only partly recoverable. Similar behaviour was observed in ABS 13. In order to investigate this effect further, dimensional measurements were made on a specimen of ABS 16, which was cycled repeatedly and continuously between 40 and  $-80^{\circ}\text{C}$ . The results of successive cooling cycles are shown in Fig. 6. During the first cooling cycle, normal, linear thermal contraction occurred between 40 and  $-20^{\circ}\text{C}$ , at which point anomalous contraction began. This non-linear behaviour continued to about  $-60^{\circ}\text{C}$ . On reheating from  $-80^{\circ}\text{C}$ , thermal expansion was basically linear. Within experimental error, the material followed the same linear path during subsequent cooling and heating cycles.

Each point in Figs. 5 and 6 provides information about the current state of cavitation in ABS 16, as already discussed in relation to Fig. 3. Points lying on the lower construction line indicate that no cavitation has taken place, while points lying on the upper construction line correspond to 100% rubber particle cavitation, involving full relaxation of internal stress. From the location of intermediate points, it is then possible to apply Eq. (1) to calculate an effective degree of cavitation, by treating the ABS as a three-component composite, with a PSAN matrix containing a volume fraction  $x\Phi_r$  of particles that are fully cavitated (i.e. they behave mechanically like voids), and a volume fraction  $(1-x)\Phi_r$  of intact, well-bonded rubber particles, where  $\Phi_r$  is the total volume fraction of rubber particles in the ABS; i.e.  $\Phi_r = 0.16$  in the case of ABS 16.

According to this interpretation, the fraction of particles that have cavitated is  $x$ . However, it must be recognised that this approach is a simplification, and that there is an alternative interpretation. The rubber particles might not be fully-relaxed, in which case the fraction of cavitated particles could be significantly larger than  $x$ . The term ‘effective degree of cavitation’ was chosen in recognition of this possibility.

Fig. 7 shows the relationship between effective degree of cavitation and temperature for ABS 16 during the first cooling–heating cycle, using the data given in Fig. 5. There is some scatter in the data, especially at higher temperatures, where the errors are inevitably larger because the construction lines converge (see Fig. 3). Nevertheless, the response of ABS to thermal cycling becomes clearer when the data are analysed in this way. During the initial cooling from 100 to  $-20^{\circ}\text{C}$ , there is little or no cavitation. Between  $-20$  and  $-50^{\circ}\text{C}$ , there is a rapid increase in the degree of cavitation, while at lower temperatures the process occurs more slowly, and eventually stops. On reheating, the effective degree of cavitation decreases linearly with increasing temperature. Similar behaviour occurs during subsequent thermal cycling, as shown in Fig. 8. Linear regression analysis of

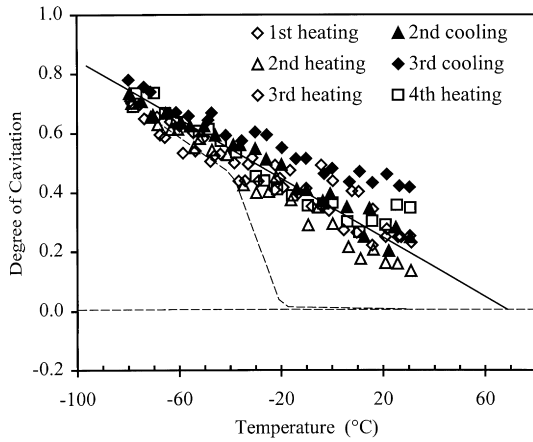


Fig. 8. Effective degree of cavitation in ABS 16 during successive cooling cycles, calculated using principle shown in Fig. 3. Dotted line shows contraction curve for first cooling test, taken from Fig. 7. Specimen was annealed after third cooling–heating cycle.

these data give intercepts on the temperature axis at  $70 \pm 10^\circ\text{C}$ .

The changes in behaviour induced by thermal cycling between  $+40$  and  $-80^\circ\text{C}$  are almost completely obliterated when the specimen is heated above the  $T_g$  of the matrix. On heating, the rubber phase expands more rapidly than the PSAN matrix, until at  $100^\circ\text{C}$  all dilatational forces acting on the particles should fall to zero, and any voids present should close up completely. To test this principle, the specimen of ABS 16 discussed above, after being subjected to three cooling–heating cycles, was annealed for one hour at  $105^\circ\text{C}$  under vacuum, then cooled slowly to  $23^\circ\text{C}$  by switching off the oven. As shown in Figs. 9 and 10, this annealing

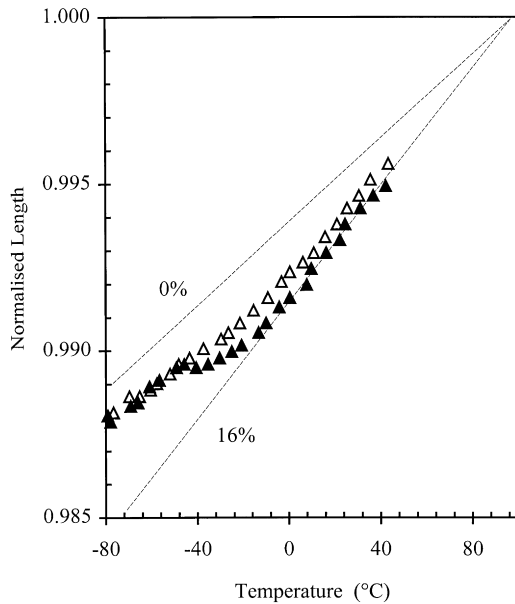


Fig. 9. Thermal contraction ( $\blacktriangle$ ) and expansion ( $\triangle$ ) behaviour of ABS 16, after repeated thermal cycling (see Figs. 5 and 6), followed by annealing at  $110^\circ\text{C}$ .

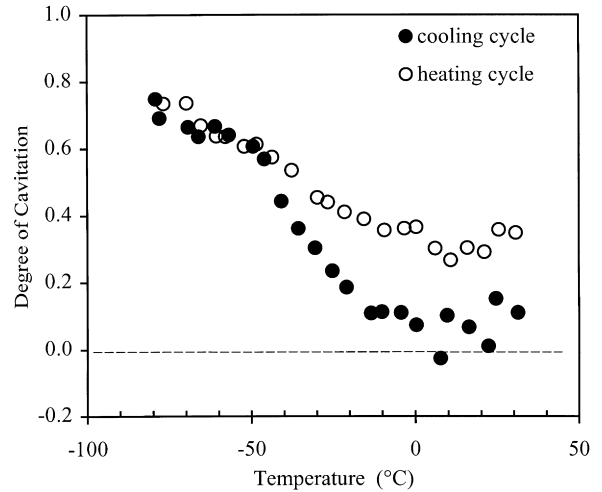


Fig. 10. Effective degree of cavitation in ABS 16 during first cooling–heating cycle after annealing, from data given in Fig. 9.

treatment has the effect of restoring the anomalous thermal contraction behaviour, albeit in slightly diminished form. Between  $+40$  and  $-20^\circ\text{C}$  thermal contraction is linear, and in approximate agreement with the predictions of Eq. (1) for an ABS containing about 14.5 vol% of intact rubber particles and 1.5% of cavitated particles. Below  $-20^\circ\text{C}$ , the rubber particles cavitate, giving rise to anomalous thermal contraction behaviour similar to that observed in the same specimen during its first cooling cycle. From Fig. 10, it is apparent that heating above  $T_{gm}$  does not completely eliminate the damage caused by thermal cycling; the results suggest that a small fraction of very small voids survives the annealing process. Nevertheless, the dominant effect of annealing is to close most of the voids sufficiently to ensure

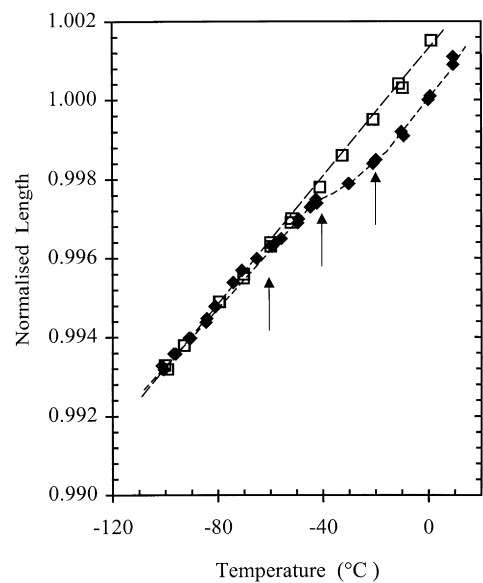


Fig. 11. Cooling ( $\blacklozenge$ ) and heating ( $\diamond$ ) curves for ABS 13 showing points at  $-20$ ,  $-40$  and  $-60^\circ\text{C}$  chosen for pre-conditioning of creep specimens.

that they reopen only when subjected to large thermally induced volume strains.

In order to explore the effects of rubber particle cavitation on large-strain mechanical properties, ABS specimens were cooled to various low temperatures, held for one hour at the chosen temperature, then warmed up and subjected to creep tests to 23°C. Because supplies of ABS 16 were limited, these experiments were carried out on ABS 13. The effects of the first cooling cycle on this polymer are illustrated in Fig. 11. Arrows at –20, –40 and –60°C identify three points on the initial curve, corresponding to the onset, middle and end of the cavitation process. The aim of the pre-cooling treatment was to induce cavitation in the rubber particles, without causing any damage to the PSAN matrix. The results of creep tests on these bars, at a temperature of 23°C and a constant applied stress of 34.5 MPa, are presented in Fig. 12. Clearly, cooling to –40 or –60°C has a profound effect on the deformation behaviour of this ABS polymer, whereas cooling to –20°C produces only modest changes in the creep rate.

Tensile creep of ABS involves two principal deformation mechanisms. Shear yielding, which is predominant at low stresses, is characterised by a decrease in creep rate with time; whereas multiple crazing, the dominant mechanism at higher stresses, shows a rapid increase in strain rate with time, after a slow start [13,14]. The shape of the creep curves, the observed whitening in the specimens during creep, and electron microscopy of microtomed and osmium-stained thin sections, all confirm that multiple crazing of the PSAN matrix and dilatation of the rubber particles are the principal mechanisms of tensile deformation. By contrast, pre-cooling ABS 27 to –60°C had no observable effect on its subsequent creep behaviour at 23°C, a result that is consistent with its approximately linear contraction behaviour, as illustrated in Fig. 1. The small deviation from linearity below 0°C indicates that levels of cavitation in ABS 27 were quite low.

#### 4. Discussion

This work has identified a method for generating and monitoring rubber particle cavitation in toughened plastics, without the complications usually involved, and has also shown how the new method can be used to investigate important aspects of behaviour related to cavitation. Unlike tensile testing, simple cooling does not produce large plastic strains in the matrix. Indeed, thermal contraction of a well-bonded rubber particle produces *compressive* tangential stresses in the surrounding matrix shell. Under appropriate conditions, especially near  $T_{gm}$ , these stresses might undergo visco-elastic relaxation, or even produce a certain amount of plastic deformation in very localised regions of high stress, but the main effect appears to be the establishment of large tri-axial tensile stresses in the rubber particles, leading to cavitation or debonding of those

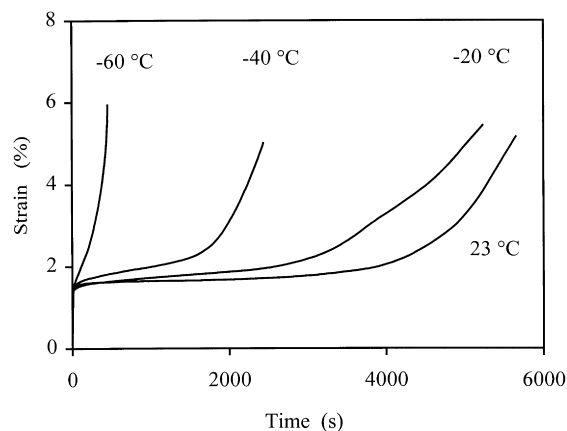


Fig. 12. Creep curves for ABS 13 at 23°C under a tensile stress of 34.5 MPa, showing the effects of pre-cooling to –20, –40 and –60°C.

particles under critical conditions [8,9]. The present study has advanced understanding in four main areas: (a) the criteria for rubber particle cavitation; (b) the role of liquids such as silicone oils in void formation; (c) methods for measuring the fraction of rubber particles that have cavitated; and (d) the effects of cavitation upon yielding in the surrounding matrix.

##### 4.1. Criteria for cavitation

The energy balance model identifies two separate criteria for rubber particle cavitation [2,8,9]. The first is purely thermodynamic; viz. the energy released during void formation must exceed the energy needed to form the void. This is a necessary condition, but whether it is sufficient is open to question. The second criterion is kinetic, and is based on the observation that the energy-balance equation predicts a maximum in the energy of a cavitated particle at small void sizes. Earlier work by Ayre and Bucknall [7] showed experimentally that rubber particles are much more resistant to cavitation than is predicted by the thermodynamic criterion, and raised the possibility that the rate of initiation of voids is limited by an energy barrier. As with other (Arrhenius-type) chemical and physical rate processes, the kinetics of conversion from one state to another are strongly dependent upon the height of the energy barrier, and the amount of thermal energy available to carry each participating element of material over the barrier.

In cavitation initiated by cooling, the height of the energy barrier is not fixed, as in the standard Arrhenius treatment, but varies with temperature. In order to understand this behaviour, it is necessary to examine the form of the energy balance equation. The simplest analysis is based on a spherical particle of radius  $R_0$ , which is subjected to a volume strain  $\Delta_V$ , thereby increasing its radius to  $R$ . If this enhanced radius  $R$  is now held constant, so that no further work is done by the matrix on the particle during the formation of a hole of radius  $r$ , the energy of the cavitated particle,  $U(r)$ , is

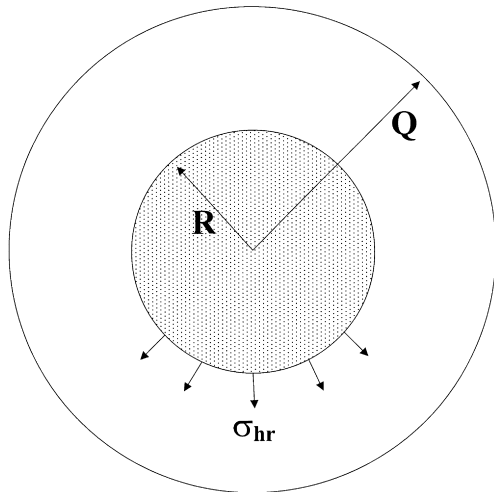


Fig. 13. Simple concentric core-shell element, used in calculating energy changes during cavitation of the rubber core.

given by:

$$U(r) = \frac{2}{3}\pi R^3 K_r \left(\Delta_V - \frac{r^3}{R^3}\right)^2 + 4\pi r^2 \Gamma_r + 2\pi r^3 G_r F(\lambda_f) \quad (3)$$

Total energy      Volumetric strain energy      Surface energy      Rubber stretching energy

where  $K_r$  is the bulk modulus of the rubber phase,  $\Gamma_r$  is its surface energy,  $G_r$  is its shear modulus, and  $F(\lambda_f)$  is a function of the failure strain in biaxial extension [8]. In practice,  $F(\lambda_f)$  can be usually assigned a value of unity. Eq. (3) predicts an energy maximum at small  $r$  because the surface energy term in  $r^2$  initially increases more rapidly than the stored energy term in  $(\Delta_V - r^3/R^3)^2$  decreases.

More accurate calculations can be made by taking due account of energy interactions between particle and matrix as the void expands. The inclusion in the analysis of work done by the matrix does not alter the general pattern of

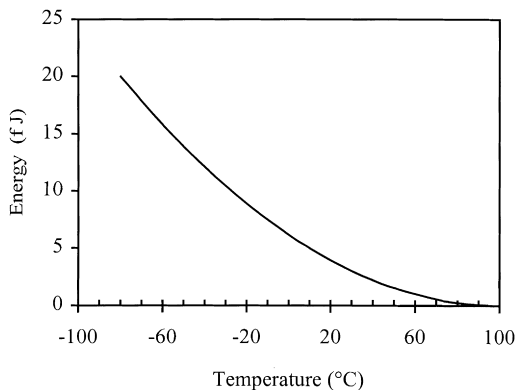


Fig. 14. Relationship, calculated using the full energy balance model, between temperature and the initial strain energy of a rubber particle with  $R = 100$  nm,  $\phi = 0.16$ . For other properties used see text. Note:  $1 \text{ fJ} = 10^{-15} \text{ J}$ .

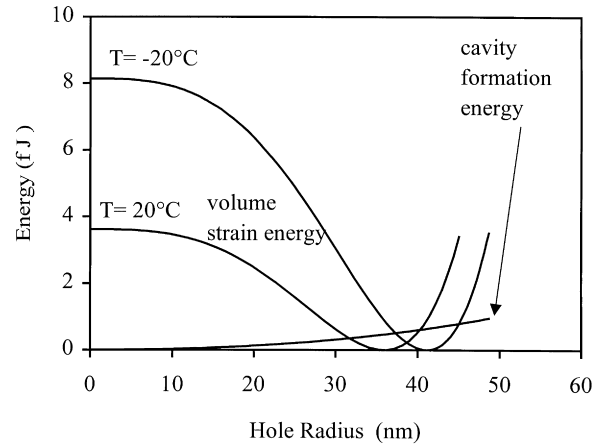


Fig. 15. Results of calculations based on the full energy-balance model with  $\Gamma_r = 20 \text{ mJ m}^{-2}$ ,  $R = 100$  nm, showing contributions from volume strain energy and cavity formation energy (surface formation plus stretching) to the total energy of a rubber particle at  $-20$  and  $+20^\circ\text{C}$ .

behaviour, but simply increases the amount of energy available for initiating a void [9]. In straightforward thermal contraction experiments, with no external stresses, the initial volume strain is directly proportional to  $\Delta T$ , the difference between the current temperature  $T$  and the solidification temperature  $T_{\text{solid}}$  of the matrix, which in ABS can be equated with the glass transition temperature  $T_{\text{gm}}$ . The hydrostatic (i.e. mean) stress in a rubber particle,  $\sigma_{\text{hr}}$ , can then be calculated using the model illustrated in Fig. 13, in which a spherical rubber particle of radius  $R$  is enclosed in a concentric spherical shell of rigid matrix, with an external radius  $Q$ . The volume fraction of rubber,  $\phi_r$ , is then  $(R/Q)^3$ , and  $\sigma_{\text{hr}}$  is given by:

$$\sigma_{\text{hr}} = \frac{(\beta_r - \beta_m)\Delta T}{\frac{1}{K_r} + \frac{4G_m\phi_r + 3K_m}{4G_m K_m(1 - \phi_r)}} \quad (4)$$

where  $G_m$  and  $K_m$  are the shear and bulk moduli of the matrix. Applying Hooke's Law,  $U_0$ , the initial volumetric strain energy density in the particle is:

$$U_0 = \frac{\sigma_{\text{hr}}\Delta V_r}{2} = \frac{\sigma_{\text{hr}}^2}{2K_r} = \frac{K_r\Delta V_r^2}{2} \quad (5)$$

Combining Eqs. (4) and (5), it can be seen that the initial stored energy available for void formation increases with  $(\Delta T)^2$ , as shown in Fig. 14.

It follows that the cavity formation energy, which is the sum of the surface energy and rubber stretching terms in Eq. (3), becomes less important as the temperature is lowered, because the curves for both the surface energy and the rubber stretching energy against hole radius are relatively insensitive to temperature, while the contribution from the stored energy curve become progressively larger on cooling. This point is illustrated schematically in Fig. 15, which shows clearly that there is more than enough energy in the



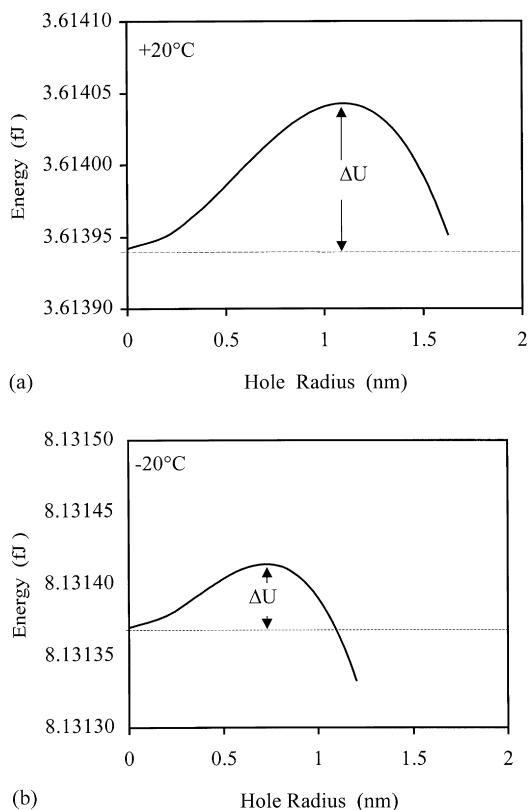


Fig. 16. Initial sections of calculated energy-void size curves based on Fig. 15, comparing energy maxima at (a) +20 and (b) -20°C.

system to cause cavitation at +20°C, according to the thermodynamic criterion. The energy minimum is well below  $U_0$  at this temperature.

The data used to generate the curves presented in Figs. 14–18 are:  $\phi_r = 0.16$ ,  $G_m$ ,  $K_m$  and  $K_p = 1.2$ , 4.0 and 2.0 GPa, respectively,  $G_r = 0.5$  MPa, and  $\Gamma_r = 20$  mJ m<sup>-2</sup>. A low value of  $\Gamma_r$  was chosen to represent a typical surface energy for silicone oil [15], on the assumption that a trace of silicone oil will act as a surfactant during cavitation, facilitating the formation of void surfaces in the

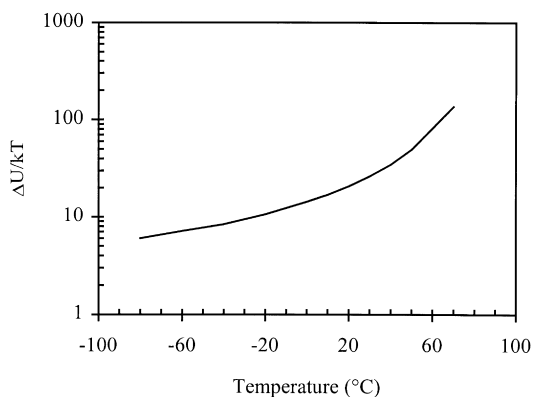


Fig. 17. Relationship, calculated using full energy balance model, between temperature and activation enthalpy for cavitation, expressed as  $\Delta U/kT$  and plotted on a logarithmic scale.

Table 1

Values of hole radius  $r$ , at the energy minimum, and the corresponding fall in potential energy,  $\Delta U/U_0$ , where  $U_0$  is the initial energy

$\Gamma$ (mJ m <sup>-2</sup> )	$r$ (nm)		$\Delta U/U_0$	
	20	35	20	35
$\phi = 0.13$	41.0	40.6	0.929	0.894
$\phi = 0.27$	40.5	40.5	0.928	0.892

rubber. In the absence of additives, polybutadiene has a surface energy of 35 mJ m<sup>-2</sup> [16].

From both Fig. 15 and Table 1, it is clear that neither surface energy  $\Gamma_r$  nor rubber content  $\phi_r$  has a significant effect on the energy minimum in the temperature range -20 to +20°C. In all cases, cavitation is accompanied by a drop of ~90% in stored energy. By contrast, there are very marked differences in the height of the energy maximum when  $\Gamma_r$  is increased from 20 to 35 mJ m<sup>-2</sup>, as shown in Table 2, or when the temperature is reduced, as illustrated in Figs. 15–17. In absolute terms, the heights of the energy barriers are very small, but they are clearly important in controlling the initiation of a void. Table 2 confirms that the addition of silicone oil, rather than a reduction in the rubber content, was the critical factor that enabled ABS 13 to cavitate spontaneously on cooling; ABS 27, which contained no silicone oil, showed only a small amount of cavitation.

The critical void size at the energy maximum also decreases on cooling, as indicated in Fig. 18. It is perhaps significant that the calculations give a critical void diameter at -20°C of approximately 1.3 nm, which is at the upper end of the range of void sizes that one might expect to be generated through ordinary ‘free volume’ effects. Somewhat smaller voids, with average diameters of 0.62 nm, have been observed in unstressed polybutadiene at -20°C, using positron annihilation lifetime analysis [17]. Even more striking comparisons can be made between the energy levels of critical voids in thermally stressed rubber particles and the ‘free volume’ voids in unstressed rubbers. Fig. 17 shows that  $\Delta U/kT \sim 10$  in ABS 16 at -20°C, where cavitation begins, and ~6.7 at -60°C, where the process appears to terminate. Taking  $\Gamma_r = 35$  J m<sup>-2</sup> for plain polybutadiene, and a ‘free volume’ radius of  $r$  as 0.25 nm, we obtain  $\Delta U/kT = 4\pi r^2 \Gamma_r/kT = 6.7$  at 23°C. It may be concluded

Table 2

Values of the hole radius  $r$ , at the top of energy barrier (energy maximum) and the corresponding activation energy,  $\Delta U$

$\Gamma$ (mJ m <sup>-2</sup> )	$r$ (nm)		$\Delta U$ (aJ) <sup>a</sup>	
	20	35	20	35
$\phi = 0.13$	0.67	1.16	0.037	0.198
$\phi = 0.27$	0.68	1.17	0.038	0.203

<sup>a</sup> 1 aJ = 10<sup>-18</sup> J

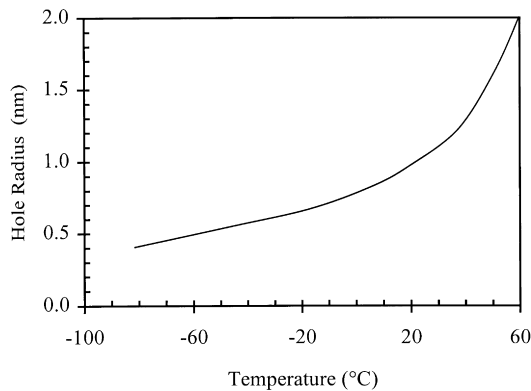


Fig. 18. Relationship between temperature and critical void radius for cavitation, calculated using full energy balance model.

that when the temperature reaches  $-20^{\circ}\text{C}$ , rubber particles containing a trace of silicone oil are able to produce a steady supply of voids large enough to cause spontaneous cavitation, and that further cooling will accentuate this effect.

On the basis of this discussion, it is reasonable to suggest that rubber particles cavitate at an appreciable rate when the energy barrier is low enough to be surmounted with the aid of available thermal and mechanical energy. Barrier heights are reduced when a dilatation is imposed on the rubber, through differential cooling or mechanical loading, or both. The analysis given above is basically an extension of Eyring's approach to stress-activated flow.

Reheating the specimen, or partial removal of the mechanical loading, does not necessarily allow the voids to close, because they are thermally stable at quite low imposed volume strains, once the energy barrier has been crossed. Calculations show that in unstressed ABS 16, minimum values of  $U(r)$  are lower than  $U(0)$  at temperatures up to about  $85^{\circ}\text{C}$ . Even above  $85^{\circ}\text{C}$ , the voids are metastable, because there is still an energy barrier to be crossed before the voids can close. Only at temperatures above (or immediately below)  $T_{\text{gm}}$  can the voids close up spontaneously. These conclusions are in good agreement with the experimental findings presented in Figs. 5–10.

Once the ABS has been annealed, and most of the voids present have therefore closed up completely, the activation energy barrier again imposes a limitation on spontaneous cavitation during cooling. Some residual damage is to be expected in the rubber phase, because the strains involved in cavitation are sufficient to cause some bond rupture in the crosslinked network, but the properties of the original ABS are largely restored. The effects of residual damage on the properties of ABS, following pre-straining and annealing, have been studied extensively by Yang [18].

Thus, both the experimental results and the modelling strongly suggest that void formation is controlled by an energy barrier, which is an intrinsic feature of the energy-balance model. The model predicts a progressive increase in the rate of void formation as the material is cooled, because the height of the energy barrier decreases as thermally

induced stresses become larger (see Fig. 17). At first sight, this conclusion appears to be paradoxical. In most standard rate processes, conversion rates increase with temperature, as the levels of thermal energy available to surmount the activation barrier become larger. However, it should be noted that supercooling effects similar to those recorded in this paper are also observed in crystallization and freezing. For example, rates of crystallization in both metals and polymers increase rapidly as the system is cooled below its melting point. The basic reasons are the same in all cases; the surface-to-volume ratio determines the height of an energy barrier.

#### 4.2. Measuring levels of cavitation

The discussion associated with Figs. 3, 7, 8 and 10 has already explained how thermal contraction or expansion data can be used to calculate the fraction of rubber particles that have cavitated. One further point can be made in relation to these measurements. At medium to high rubber contents, cavitation of the rubber particles results in a very large drop in  $\beta_{\text{tp}}$ , the volumetric coefficient of expansion of a toughened plastic, as predicted by Eq. (1) and illustrated in Fig. 3. It should therefore be possible to determine the extent of rubber particle cavitation in a toughened polymer simply by determining its thermal expansion coefficient, provided that the expansion measurements are reasonably accurate, and the rubber content of the polymer is known. Thus thermal contraction and expansion measurements constitute a non-invasive method for detecting particle cavitation in rubber-toughened polymers. Unlike light scattering, the method is applicable to opaque materials. Where the material has already been subjected to stress- or temperature-cycling, measurements of  $\beta_{\text{tp}}$  are in principle sufficient to determine whether cavitation has already taken place. The one limitation of the method is that the rubber concentration must be high enough to produce a measurable change in  $\beta_{\text{tp}}$  when the rubber particles are intact.

While anomalous thermal contraction behaviour is not observed in all ABS polymers, it is exhibited by a number of them. The preferred conditions are similar to those responsible for splitting of the low temperature loss peak in ABS: the presence of very small amounts of a liquid with a low surface energy, preferably combined with a medium to low concentration of rubber. There is obvious scope for applying the principles described in this paper to a number of important problems relating to rubber toughening.

#### 4.3. Effects of cavitation on yielding in ABS

Another important outcome of this programme is the information that it provides about yielding in cavitated rigid polymers. It is relatively easy to prepare specimens in which the rubber particles have already cavitated, without at the same time producing plastic deformation in the matrix. The availability of such specimens is of considerable value in designing experiments to study rubber particle

cavitation, for example to determine whether or not cavitation precedes yielding or multiple crazing in toughened plastics. The method has one major limitation, namely, that it is applicable only to materials that undergo cavitation between room temperature and the  $T_g$  of the rubber phase. Nevertheless, it offers two significant benefits: (a) samples with defined levels of rubber particle cavitation can be prepared in advance of mechanical testing, so that the effects of voids can be distinguished from those due to other deformation processes in the toughened polymer; and (b) cavitation can be induced homogeneously in specimens of irregular shape.

The effects of pre-formed voids on the creep of ABS are very significant. There is already some evidence that cavitation of the rubber particles is a necessary pre-cursor to multiple crazing in the matrix of ABS and high-impact polystyrene (HIPS). However, most of the evidence is indirect and inconclusive, and there is an urgent need to obtain more information on the subject. The creep experiments outlined above provide strong evidence that particle cavitation initiates multiple crazing, rather than the other way around.

The data presented in Fig. 12 show that a stress of 34.5 MPa is sufficient to initiate crazing even in specimens that have not been pre-cooled. Thus, pre-cooling causes quantitative rather than qualitative changes in the behaviour of ABS creep specimens; the presence of cavitated particles in large concentrations results in a substantial increase in creep rate, but without altering the shapes of the creep curves.

The obvious explanation for this behaviour is that pre-cooling progressively increases the number of sites (i.e. cavitated rubber particles) that are able to initiate crazes when a sufficiently large stress is applied. In samples that have not been cooled below 23°C, the number of such sites is relatively small, and times in the order of 4000 s are needed for the crazes initiated at these sites to increase in area and link up with other, co-planar crazes. Only when this stage has been reached, and the constraints imposed by the surrounding PSAN matrix have thereby been removed, does the strain rate reach the relatively high values recorded in Fig. 12 for creep strains above 2%. Crazing is an activated process, which follows the Eyring equation, and the overall creep rate is determined not only by the number of craze initiation sites, but also by the applied stress and test temperature.

## 5. Conclusions

This work has shown that spontaneous cavitation can take place in the rubber phase of ABS when specimens are cooled below room temperature, and that cavitation is strongly promoted by silicone oil, because of its low surface energy. In the absence of cavitation, differential thermal contraction generates triaxial tension in the rubber particles

and causes a large increase in the coefficient of thermal expansion of ABS relative to that of the parent polymer, PSAN. The energy required to form voids in the rubber phase is thus generated by differential thermal contraction. Cavitation causes relaxation in the strained rubber, and hence an expansion of the ABS, which results in an S-shaped contraction vs temperature curve.

On reheating, and in subsequent cooling–heating cycles, the volume-temperature curve is linear, provided that the specimen has not been heated above the  $T_g$  of the matrix during thermal cycling. It is concluded that rubber particle cavitation is a thermally activated rate process, controlled by an energy barrier. Calculations based on the Lazzeri–Bucknall energy balance model [2,8,9] confirm that the height of the energy barrier (representing an activation energy) decreases dramatically on cooling to –20°C, and that the critical void size at the energy maximum is then approximately 1 nm, which is comparable with the void sizes that constitute the free volume in a rubber.

This work has also shown that it is possible to estimate the fraction of rubber particles that have cavitated on cooling, by analysing volume–temperature curves for ABS, and that the presence of voids in the rubber particles leads to a substantial increase in creep rates.

## Acknowledgements

The authors thank Bayer AG for permission to publish this paper, and EPSRC (GR/K24703) for financial support for DSA.

## References

- [1] Bascom WD, Cottingham RL, Jones RL, Peyser P. *J Appl Polym Sci* 1975;19:2545.
- [2] Lazzeri A, Bucknall CB. *Polymer* 1995;36:2895.
- [3] Bucknall CB. In: Haward RN, Young RJ, editors. *The physics of glassy polymers*, 2. London: Chapman & Hall, 1997.
- [4] Brandrup J, Immergut EH. *Polymer handbook*, 3. New York: Wiley, 1989.
- [5] Bayer AG. *Plastics business group, CAMPUS 4.0 Database* 8/97.
- [6] Boyce ME, Argon AS, Parks DM. *Polymer* 1987;28:1680.
- [7] Ayre DS, Bucknall CB. *Polymer* 1998;39:4785.
- [8] Lazzeri A, Bucknall CB. *J Mater Sci* 1993;28:6799.
- [9] Bucknall CB, Karpodinis AM, Zhang XC. *J Mater Sci* 1994;29:3377.
- [10] Humme G, Kranz D, Morbitzer L, Ott KH. *J Appl Polym Sci* 1976;20:2691.
- [11] Morbitzer L, Humme G, Ott KH, Zabrocki K. *Angew Makromol Chem* 1982;108:123.
- [12] Booiij C. *Brit Polym J* 1977;March:47.
- [13] Bucknall CB, Drinkwater IC. *J Mater Sci* 1973;8:1800.
- [14] Bucknall CB. *Toughened plastics*, London: Applied Science, 1977 p. 215.
- [15] Merck, *Laboratory Supplies Catalogue*, p2-585, 1998.
- [16] Edwards DC. *J Mater Sci* 1992;25:4175.
- [17] Bartoš J, Bandzuch P, Šauša O, Křištiaková K, Křištiák J, Kanaya T, Jenninger W. *Macromolecules* 1997;30:6906.
- [18] Yang HH. *PhD Thesis*, Cranfield University, 1997.